World Academy of Science, Engineering and Technology
International Journal of Aerospace and Mechanical Engineering
Vol:18, No:1, 2024

Failure Analysis of a 304 Stainless Steel Flange Crack at Pipeline Transportation of Ethylene

Parisa Hasanpour, Bahram Borooghani, Vahid Asadi

***Abstract*—**In the current research, a catastrophic failure of a 304 stainless steel flange at pipeline transportation of ethylene in a petrochemical refinery was studied. Cracking was found in the flange after about 78840h service. Through the chemical analysis and tensile tests, in addition to microstructural analysis such as optical microscopy and Scanning Electron Microscopy (SEM) on the failed part, it found that the fatigue was responsible for the fracture of the flange, which originated from bumps and depressions on the outer surface and propagated by vibration caused by the working condition.

***Keywords*—**Failure analysis, 304 stainless steel, fatigue, flange, petrochemical refinery.

I. Introduction

STAINLESS steel is popular in many industries such as oil and gas, automotive, and medical industries. The popularity of stainless steel can be attributed to its ability to resist corrosion, withstand high stress, and operate at high temperatures. Among all types of stainless steel, the austenitic stainless steel type 304 is commonly used [1]-[10].

Flanges are generally used for parts transfer to facilitate disassembly and assembly in industries like refineries and fastened together by bolts. In general, used materials for pipe and equipment flange are Q235, 20 steel, 16Mn, 304, 316, and 316L.

Recently, several studies have been reported by many researchers about stainless steel 304 failures. Pelliccione et al. [11] studied failure analysis of a stainless steel socket-welding flange and concluded that improper manufacturing process and chemical composition has led to failure. Lu et al. [12] also investigated the premature damage of a 304 stainless steel flange. The results revealed that improper welding operation led to defect formation and crack propagated circumferentially in the weld seam. Zhang et al. [13] analyzed a failure of hand-hole flange cracking. The results showed that cracking was caused by sensitization and liquation crack due to low-melting-point annular oxide inclusions and silicate eutectic. Moreover, Pastocic et al. [14] investigated a coil spring failure. It proved that the continuous contact between the coils resulted in corrosion pits, which were considered crack initiation points, consequently leading to the final fracture. The obtained results from the stress analysis by finite element model of coil spring give a prediction of the spring fatigue life. Vukelic et al. [15] studied the failure of a crane gear damage. The results showed that subsurface material inclusions served as initiation points for cracks. Additionally, excessive stress that provoked crack propagation was probably due to gear shafts misalignment resulting in teeth mismatch.

In the current study, to avoid the financial losses and shut down due to probably failure of an engineering part, failure analysis of an 8 in. 304 stainless steel flange was carried out. The flange has been used in the transportation pipeline of ethylene in a petrochemical company by conditions listed in Table I.

TABLE I
THE OPERATING CONDITIONS OF THE FAILED FLANGE

Operating pressure (bar)	Operating temperature (°C)	Exposure time (h)	Oscillating rate (mm/s)	Fluid's mass flow (kg/h)
3.8-5.8	53-58	78840	14	H_2: 34.69 C_2H_4: 5999.13 C_2H_6: 1063.37 C_4H_8: 683.14 N_2: 21075.31 Hexane: 11248.78

II. Experimental Procedures

Firstly, visual inspection and liquid penetrant testing according to ASME SEC V were carried out on the flange to determine the type, amount, and location of the failure. Next, the chemical composition (by Optical Emission Spectroscopy (OES)) of the 304 stainless steel flange was investigated as well as tensile testing (according to ASTM A182, by Santam Universal testing machine). Moreover, the fracture surface of the failed flange was prepared for investigation using both stereo optical microscope and scanning electron microscope (SEM) (by Philips XL30 Scanning electron microscopy). Also, Energy dispersive spectroscopy (EDS) was used to characterize the chemical constituents in the metallographically prepared samples of the cross-section of the flange.

III. Results and Discussions

As shown in Fig. 1, the penetration testing result of the damaged flange reveals an 80 mm crack in the deformed part of the flange. Also, a closer visual examination shows that the cracking propagated from the internal surface through the wall. After crack initiation, the cracking has propagated through the thickness of the flange. Plus, in the outer surface of the part some circumferential bumps and depressions on the outer

Parisa Hasanpour is Senior Metallurgy engineer, Corrosion Laboratory, Consulting Engineers of Azmouneh Foulad Company, Isfahan, Iran
Bahram Borooghani is Senior Technical Inspector, Technical Inspection Office, East Oil & Gas Production Co. (EOGPC), Sarakhs, Iran (*corresponding author, phone: +989158714561, e-mail: Bahramborooghani@gmail.com).
Vahid Asadi is Senior Technical Inspection engineer, Operation Department, Fars Province Gas Company.

surface were observed which seems they stemmed from the production (machinery) process.

According to ASTM A182, to investigate the grade of the flange, chemical composition (OES test) and tensile test results of the material are needed. These tests were performed and results are provided in Tables II and III, respectively. The given results confirmed that standard alloy composition complies with the alloy composition of the flange given in Table II.

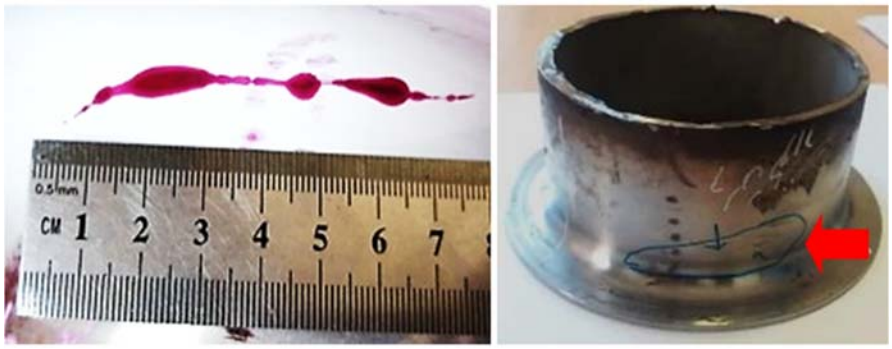

Fig. 1 Detected crack in the damaged flange (arrow)

TABLE II
CHEMICAL COMPOSITION OF THE DAMAGED FLANGE AND STANDARD REQUIREMENTS

Element	(wt%)	Stainless steel grade 304 according to ASTM A182 (wt%)
C	0.0584	0.08 max
Cr	18.8	18.0-20.0
Ni	8.10	8.0-11.0
N	0.0763	0.1 max
Mn	1.04	2.0 max
Si	0.453	1.00 max
P	0.0296	0.045 max
S	0.0057	0.030 max

TABLE III
TENSILE PROPERTIES DATA FOR FLANGE AND STANDARD REQUIREMENTS

Specimen	U.T.S. (N/ mm^2)	Y.$S_{0.2\%}$ (N/ mm^2)	Elongation (%)
1	680	231	58.2
2	695	221	58.4
3	665	235	57.6
Average	680	229	58.2
AISI 304 according to ASTM A182	515 min	205 min	30 min

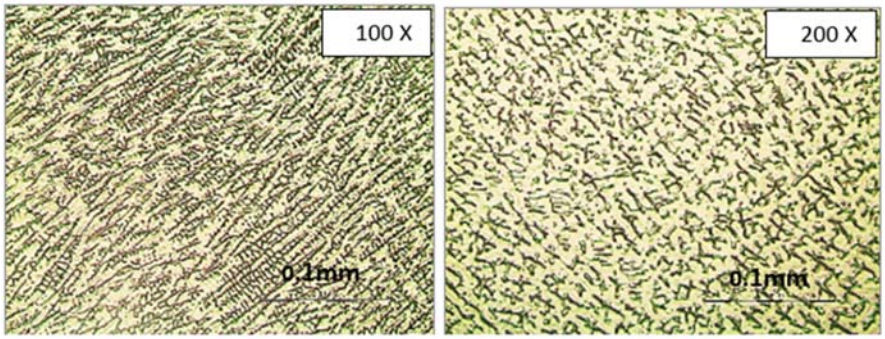

Fig. 2 The microstructure of the weld zone

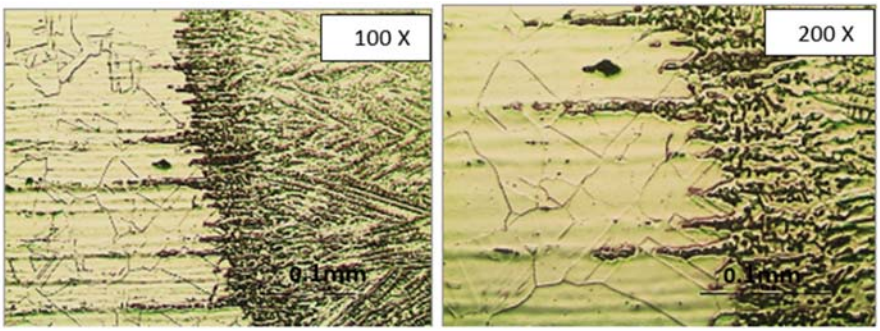

Fig. 3 The microstructure of fusion line

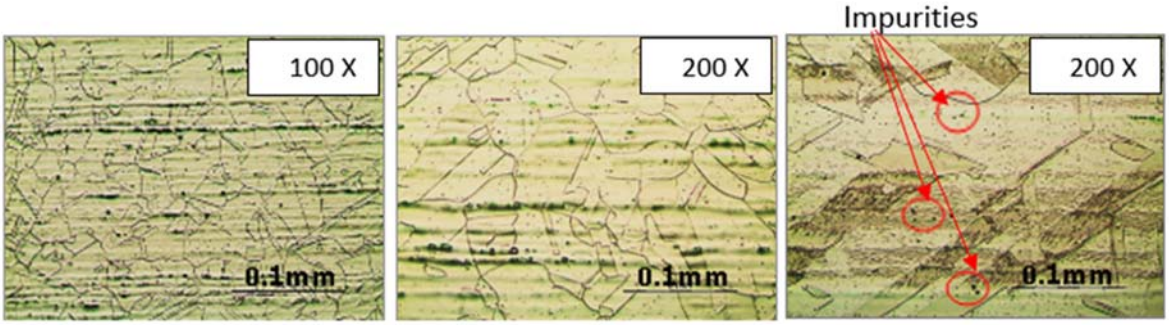

Fig. 4 The microstructure of base metal

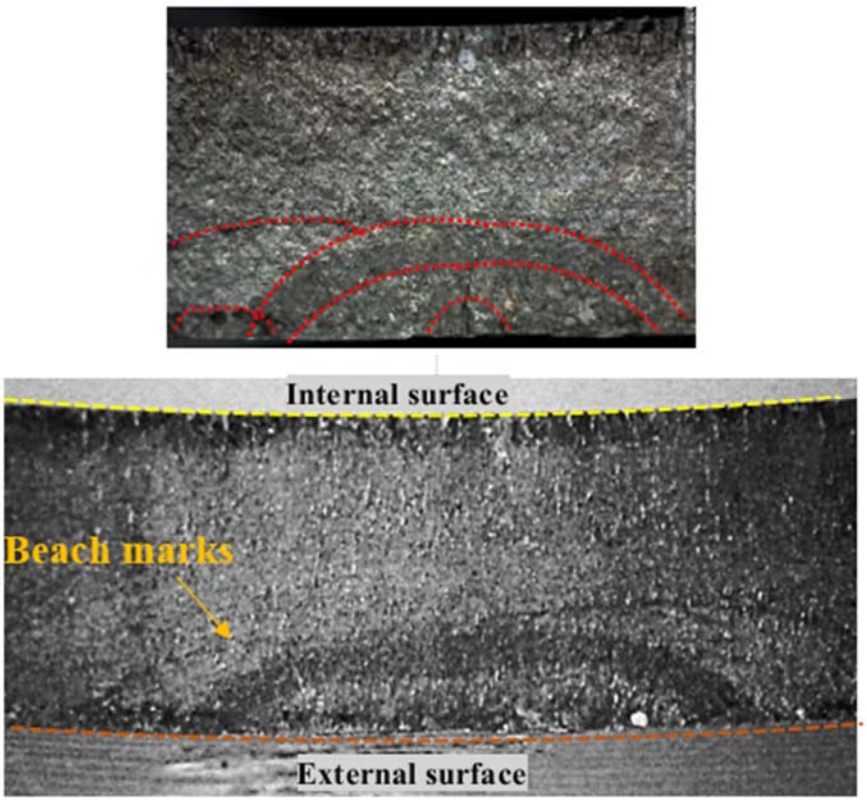

Fig. 5 The stereo microscopic images of the fracture surface

To investigate the microstructure of the flange, specimens were cut from a section of the flange just near the premature crack by wire-cutting. The samples were mounted in Epoxy and polished to a mirror finish using emery papers up to 2400 grit followed by final polishing using 0.05 μm alumina powder. Then, they immediately etched via concentrated nitric acid. Fig. 2 shows the metallographic images of the weld zone and Figs. 3 and 4 show the metallographic images of the fusion line and the base-metal, in turn. Microscopic examination revealed that the weld area has no welding defects and is composed of a combination of two phases of delta ferrite and austenite, while the base metal microstructure consists of austenite grains in which a large number of twins and strain lines resulting from the production process can be seen [16]. Besides, some impurities are observed in the microstructure.

The fracture surface was examined by stereo-microscope. Taken images showed that the fracture surface was approximately smooth. Besides, as highlighted in Fig. 5 (the red dotted line), some arc features clarified that could be beach marks resulted from fatigue phenomenon [17]. Since the flange was operated in a situation in which nearly high vibration existed (Table I), occurrence of fatigue is predictable. Moreover, the different orientations of the arcs indicated the presence of various fatigue sources [18], [19]. Since the center of the beach marks depicts the crack origin [20], it should be noted that all of the fatigue cracks initiated from external surface. As mentioned earlier, on the outer surface of the flange, just close to crack, some bumps and depressions resulted from poor finishing were observed. These regions are capable of performing as fatigue crack origins because of stress concentration [21]. Researchers also reported that there is a direct relationship between surface smoothness and fatigue life.

Therefore, surface roughness can develop fatigue in a situation which cyclic stress are existed [21]-[23].

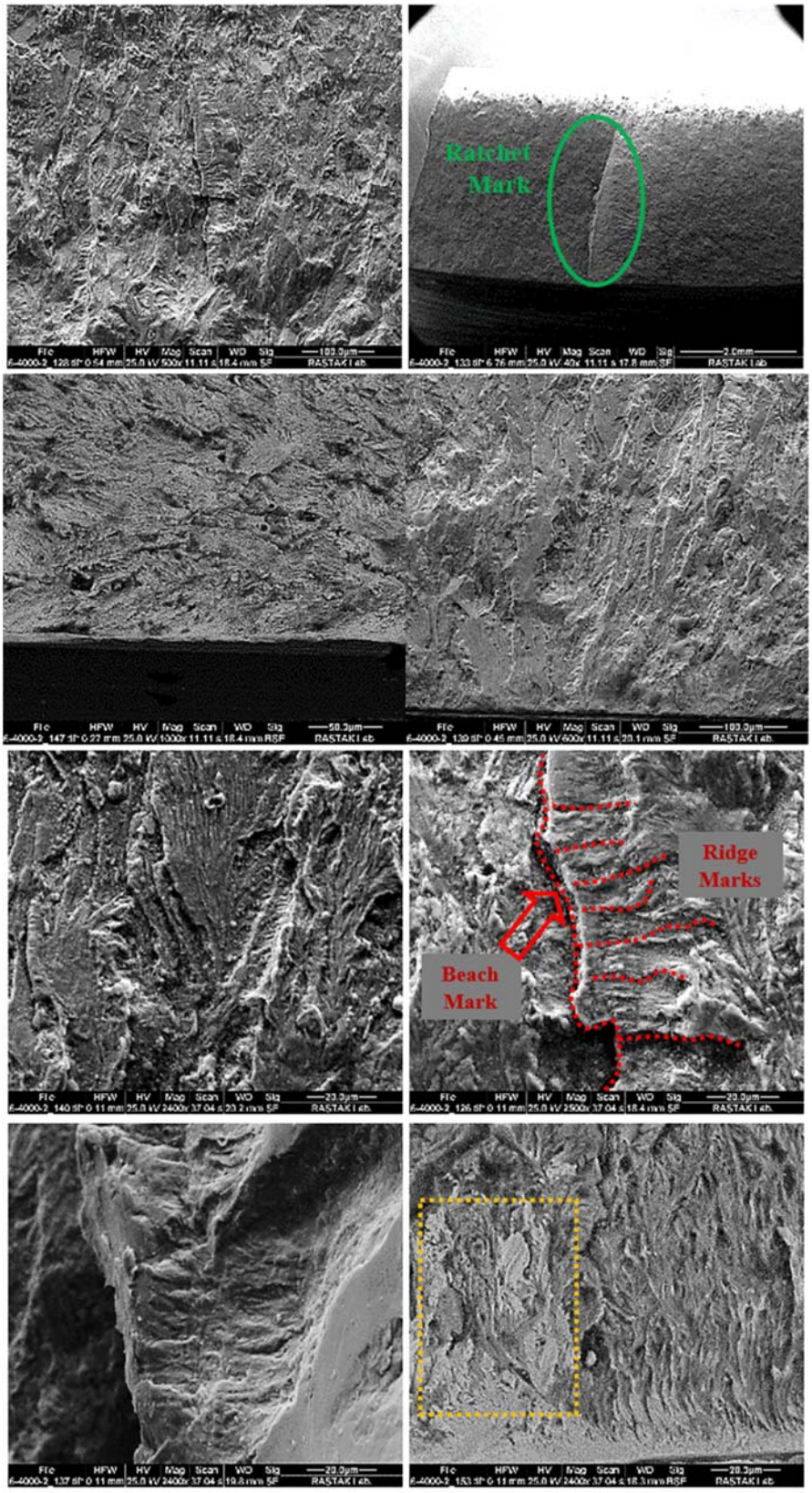

Fig. 6 The SEM images of the fracture surface

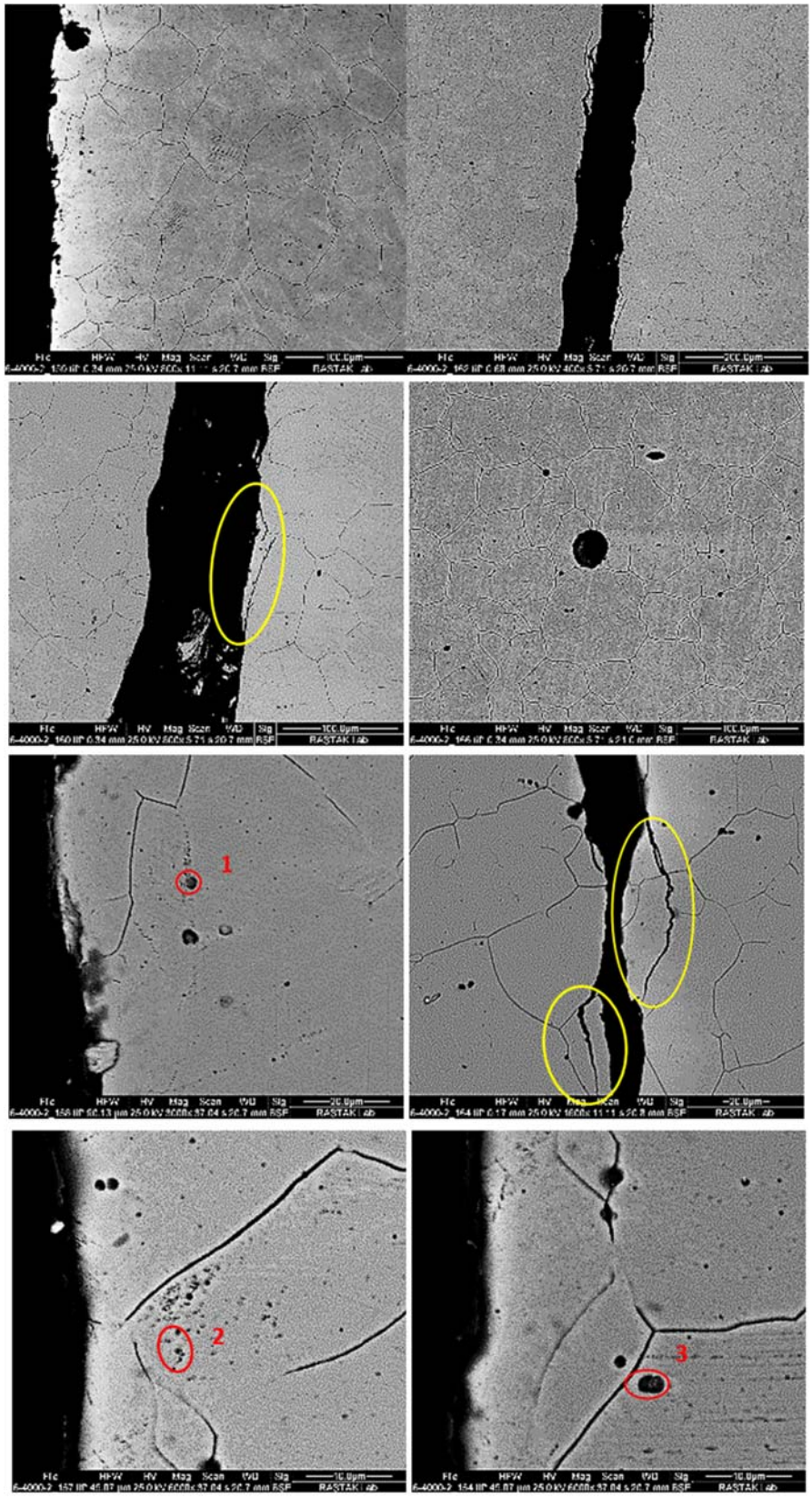

Fig. 7 SEM from the crack and the microstructure

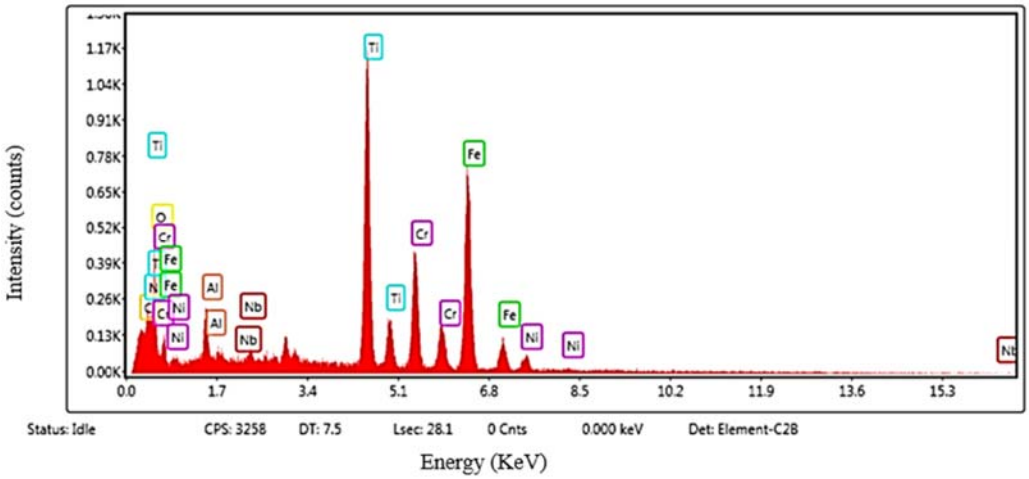

Fig. 8 EDS from point 1

The fracture surface was studied by SEM, too. The beach and ridge marks in the SEM images in Fig. 6 revealed that the fatigue phenomenon was the main reason for the crack initiation. Furthermore, the micro-cracks observed showed that the fatigue phenomenon had been dynamic and progressive in the third dimension. It could be noted that the beach marks form as a curve around the crack source, whereas the ridge marks generate just along with the crack source [24]-[26].

As mentioned above, the microscopic studies confirmed the presence of several fatigue sources mostly near the external surface.

When several fatigue sources exist in the specimen, not only do the ridge marks appear along with the crack source (perpendicular to beach marks), but also form between two beach marks produced by two different sources and result in the propagation of the integrated crack [18], [19]. The investigation of SEM images near the flange surface determined that the closer to the flange surface the wider cleavage surfaces (the orange rectangle in SEM image in Fig. 6) occur which is evidence for higher stress on the flange surface [27]. Thus, the stepwise surface (highlighted by the green oval in the SEM image in Fig. 6) which was named the Ratchet mark, was observed in the failed flange, because the stress concentration was high in the zone or thermal cycle was exerted on the specimen [18]. But in this case, the first scenario is more probable since, in the operation condition, temperature has been varied between 53-58 °C.

Finally, to investigate the crack propagation in the base metal, a specimen such as the crack tip was chosen from the flange and microscopically studied. Fig. 7 represents the SEM images of the specimen along with the crack including microstructure and impurities. The images showed austenite microstructure with some impurities that the EDS results of these points shown in Figs. 8-10 and Tables IV-VI. These impurities include carbonitride, Si, alumina, and S, generally which are typical in stainless steels. As can be seen in SEM images, these impurities are small in size and sphere in shape and because of that, it seems that they were benign for the specimen fatigue life [28]. The crack branches are shaped very thin and direct (denoted by yellow-ovals). They were also transgranular and did not propagate along with inclusions which proved the non-destructive nature of existence impurities.

TABLE IV
EDS ANALYSIS RESULTS OF POINT NO.1 IN FIG. 8

Element	Atomic (%)	wt%
C K	18.95	8.09
N K	9.75	4.85
O K	32.46	18.46
AlK	4.07	3.91
NbL	0.02	0.05
TiK	12.6	21.45
CrK	6.46	11.94
FeK	14.41	28.6
NiK	1.27	2.65

TABLE V
EDS ANALYSIS RESULTS OF POINT NO.2 IN FIG. 9

Element.	Atomic (%)	Wt%.
O K	5.63	1.71
SiK	1.34	0.71
CrK	18.5	18.25
FeK	67.55	71.55
NiK	6.99	7.78

TABLE VI
EDS ANALYSIS RESULTS OF POINT NO.3 IN FIG. 10

Element.	Atomic (%)	Wt%.
O K	8.99	2.94
AlK	2.16	1.19
SiK	0.6	0.34
S K	8.34	5.46
TiK	4.1	4.01
CrK	15.74	16.7
FeK	50.95	58.08
NiK	5.46	6.55
CuK	3.66	4.74

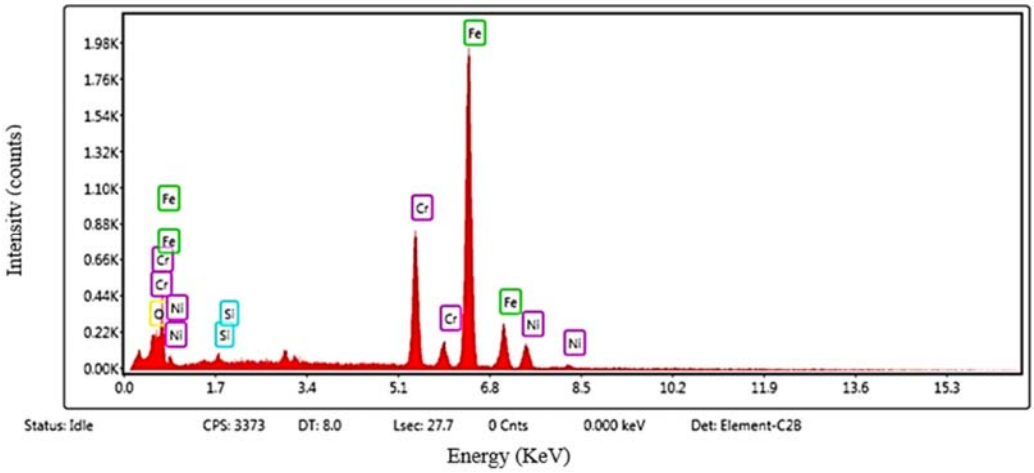

Fig. 9 EDS from point 2

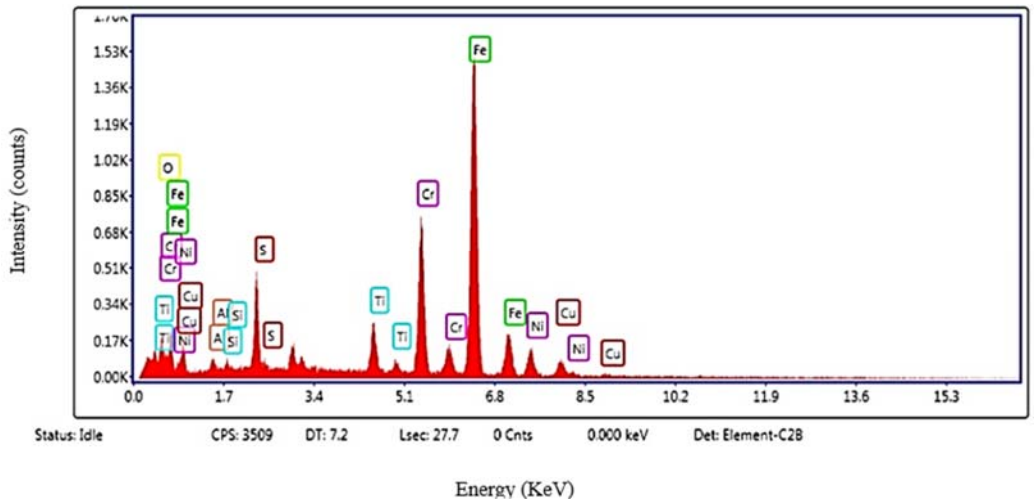

Fig. 10 EDS from point 3

IV. Conclusions

The tensile test and chemical analysis results revealed that the material was fully conformed by stainless steel 304. The metallographic data showed that the flange microstructure includes a base with austenite, twins and strain lines, and some impurities. Investigations on the crack surface using stereo microscopy proved that the beach mark formed on the crack surface with various orientations that indicates the existence of several fatigue sources in the structure.

Besides, in SEM images of the crack surface, all signs of the fatigue phenomenon such as beach marks, ridge marks, and stepwise surface were observed that confirmed that the main reason for the premature failure was the fatigue phenomenon. It should be noted that inadequate finishing of the flange external surface led to fatigue crack initiation and cyclic load due to high range vibration of working conditions propagated formed cracks.

V. Recommendations

To prevent a similar failure, it is suggested that the applied stresses to the material should be decreased. Moreover, to prevent and control the fatigue phenomenon, it is recommended to use more clean steel (with a low amount of impurities) and suitable surface finishing.

Acknowledgment

The authors would like to thank East Oil and Gas Production Company (EOGPC) for technical support.

References

[1] Marques, S.C.; Rezende, J.d.G.O.S.; Alves, L.A.D.F.; Silva, B.C.; Alves, E.; Abreu, L.R.D.; et al. (2007). "Formation of biofilms by Staphylococcus aureus on stainless steel and glass surfaces and its resistance to some selected chemical sanitizers". Brazilian Journal of Microbiology, Vol. 38, p.538-43.

[2] Wright, R.; (1976). "The high cycle fatigue strength of commercial stainless steel strip". Materials Science and Engineering. Vol. 22, pp.223-230.

[3] Lei, L-P.; Hwang, S-M.; Kang, B-S.; (2001). "Finite element analysis and design in stainless steel sheet forming and its experimental comparison". Journal of Materials Processing Technology. Vol. 110, pp. 70-7.

[4] Ha, T.K.; Jeong, H.T.; Sung, H.J.; (2007). "High temperature bending fatigue behavior of stainless steels for automotive exhaust". Journal of Materials Processing Technology. Vol. 187–188, pp. 555-8.

[5] Shah, L.H.; Akhtar, Z.; Ishak, M.; (2013). "Investigation of aluminum-stainless steel dissimilar weld quality using different filler metals".

International Journal of Automotive and Mechanical Engineering. Vol. 8, pp. 1121-31.

[6] Jamil, W.; Aripin, M.; Sajuri, Z.; Abdullah, S.; Omar, M.; Abdullah, M.; et al. (2016). "Mechanical properties and microstructures of steel panels for laminated composites in armoured vehicles. International Journal of Automotive and Mechanical Engineering". Vol. 13(3), pp. 3742-53.

[7] Lee, S.; Kim, H.; Yun, D-J.; Rhee, S-W.; Yong, K.; (2009). "Resistive switching characteristics of ZnO thin film grown on stainless steel for flexible nonvolatile memory devices". Applied Physics Letters. Vol. 95.

[8] Al-Bakri1, A.A.; Sajuri1, Z.; Abdulrazzaq, m.; Ariffin, a.k.; Fafmin, M.S.; (2017). "Fatigue properties of strained very thin 304 stainless steel sheets". International Journal of Automotive and Mechanical Engineering, Vol. 14, Issue 2 pp. 4171-4182.

[9] Yan, Li.; (2012). "Fatigue crack initiation (in 304L steel): influence of the microstructure and variable amplitude loading". Other. Ecole Centrale Paris, English. NNT: 2012ECAP0015, tel-00697002.

[10] Vickova, I.; Jonsta, P.; Vanova, P.; Kolova, T.; (2016). "Corrosion Fatigue of Austenitic Stainless Steels for Nuclear Power Engineering". Metals. Vol. 6, 319.

[11] Pelliccione, A.S.; Coelho, P.C.; Lopes, D.E.B.; Ennes, C.S.B.; Jambo, H.C.M.; Santanna, R.; (2020). "Failure analysis of a stainless steel socket-welding flange due to improper manufacturing process and chemical composition". Engineering Failure Anslysis. Vol. 108.

[12] Lu, J. S.; Xuan, H. F.; Xue, J.; (2015). "Failure Analysis of a 304 Stainless Steel Flange". Advanced Materials Research. Vol. 1120–1121, pp. 1024–1028.

[13] Zhang, Y.; Shang, X.; Song, M.; Sun, Zh.; Zhu, Sh.; (2019). "Failure analysis of handhole flange cracking". Engineering Failure Anslysis. Vol. 96, pp. 100-08.

[14] Pastorcic, D.; Vukelic, G; Bozic, Z; (2019). "Coil spring failure and fatigue analysis". Engineering Failure Analysis, Vol. 99, PP. 310-318, doi: 10.1016/j.engfailanal.2019.02.017.

[15] Vukelic, G; Pastorcic, D.; Bozic, Z; (2020). "Failure investigation of a crane gear damage". Engineering Failure Analysis, Vol. 115, 104613 doi: 10.1016/j.engfailanal.2020.104613.

[16] Zatkalíková, V.; Markoviová, L.; (2019). "Corrosion resistance of electropolished AISI 304 stainless steel in dependence of temperature". Materials Science and Engineering, Vol. 465. doi:10.1088/1757-899X/465/1/012011.

[17] Furuya, Y.; (2016). "Small internal fatigue crack growth rate measured by beach marks". Material science and engineering: A.Vol. 678, pp. 260-66.

[18] Sachs, P.E.; (2005)." Understanding the Surface Features of Fatigue Fractures: How They Describe the Failure Cause and the Failure History". ASM International: Journal of Failure Analysis and Prevention. Vol. 5(2).

[19] Zhu, Y.; Wang, Y.; Huang, Y.; (2014). "Failure analysis of a helical compression spring for a heavy vehicle's suspension system". Engineering failure analysis, Vol. 2. Pp. 169-173.

[20] Yue, J; Yan, D; Soares, G; (2018). "An experimental-finite element method based on beach marks to determine fatigue crack growth rate in thick plates with varying stress states". Engineering Fracture Mechanics. Vol. 196, pp. 123-141.

[21] Singh, K; Sadeghi, F; Correns, M; Blass, T; (2019). "A microstructure based approach to model effects of surface roughness on tensile fatigue". International Journal of Fatigue. Vol. 129. https://doi.org/10.1016/j.ijfatigue.2019.105229

[22] Gockel, J; Sheridan, L; Koerper, B; Whip, B; (2019). "The influence of additive manufacturing processing parameters on surface roughness and fatigue life". International Journal of Fatigue. Vol. 124. pp. 380-388.

[23] Lai, J; Huang, H; Buising, W; (2016). "Effects of microstructure and surface roughness on the fatigue strength of high-strength steels". Procedia Structural Integrity. Vol. 2. pp. 1213-1220.

[24] Lund, R. A.; Sheybany, Sh.; (2002). "Fatigue fracture appearances". Failure analysis and prevention. Vol. 11.

[25] Russell, A.L.; Sheybani, Sh.; (2002). "Failure analysis and prevention". ASM handbook, Vol. 11. DOI: https://doi.org/10.31399/asm.hb.v11.a0003539.

[26] Bhaumik, S.K.; Rangaraju, R.; Venkataswami, M.A.; Bhaskaran, T.A.; Paramewara, M.A.; (2002). "Fatigue fracture of crankshaft of an aircraft engine". Engineering failure analysis journal, Vol. 9, pp. 255-263.

[27] Furuya, Y.; (2019). "Gigacycle fatigue in high strength steels". Science and Technology of Advanced Materials. Vol. 20 (1), pp. 643-56.

[28] Zhang, J; Li, S.X; Yang, Z.G; Li, G.Y; Hui, W.J; Weng, Y.Q; (2007). "Influence of inclusion size on fatigue behavior of high strength steels in the gigacycle fatigue regime." International Journal of Fatigue. Vol. 29. pp. 765-771.